Genome-wide transcriptomic analyses provide insights into the lifestyle transition and effector repertoire of *Leptosphaeria maculans* during the colonization of *Brassica napus* seedlings

PARHAM HADDADI[1],[†], LISONG MA[1],[†], HAIYAN WANG[1,2] AND M. HOSSEIN BORHAN[1],[*]

[1]*Agriculture and Agri-Food Canada, Saskatoon Research Centre, 107 Science Place, Saskatoon, SK, Canada, S7N 0X2*
[2]*Center of Plant Disease and Plant Pests of Hebei Province, College of Plant Protection, Agricultural University of Hebei, Baoding, China, 071001*

SUMMARY

Molecular interaction between the causal agent of blackleg disease, *Leptosphaeria maculans* (*Lm*), and its host, *Brassica napus*, is largely unknown. We applied a deep RNA-sequencing approach to gain insight into the pathogenicity mechanisms of *Lm* and the defence response of *B. napus*. RNA from the infected susceptible *B. napus* cultivar Topas DH16516, sampled at 2-day intervals (0–8 days), was sequenced and used for gene expression profiling. Patterns of gene expression regulation in *B. napus* showed multifaceted defence responses evident by the differential expression of genes encoding the pattern recognition receptor CERK1 (chitin elicitor receptor kinase 1), receptor like proteins and WRKY transcription factors. The up-regulation of genes related to salicylic acid and jasmonic acid at the initial and late stages of infection, respectively, provided evidence for the biotrophic and necrotrophic life stages of *Lm* during the infection of *B. napus* cotyledons. *Lm* transition from biotrophy to necrotropy was also supported by the expression function of *Lm* necrosis and ethylene-inducing (Nep-1)-like peptide. Genes encoding polyketide synthases and non-ribosomal peptide synthetases, with potential roles in pathogenicity, were up-regulated at 6–8 days after inoculation. Among other plant defence-related genes differentially regulated in response to *Lm* infection were genes involved in the reinforcement of the cell wall and the production of glucosinolates. Dual RNA-sequencing allowed us to define the *Lm* candidate effectors expressed during the infection of *B. napus*. Several candidate effectors suppressed *Bax*-induced cell death when transiently expressed in *Nicotiana benthamaina* leaves.

Keywords: blackleg, canola, defence, effector, *Leptosphaeria maculans*, RNA-sequencing.

Correspondence: E-mail: hossein.borhan@agr.gc.ca
†These authors contributed equally to this work.

INTRODUCTION

Blackleg disease is a major cause of yield losses on oilseed rape canola (*Brassica napus*), the second largest oilseed crop in the world. The disease is caused by the hemibiotrophic fungus *Leptosphaeria maculans* (*Lm*), which belongs to the Dothideomycete class of ascomycetes (West *et al.*, 2001). Infection begins with the germination of ascospores (primary source of infection) and asexual spores (pycnidiospores) on the cotyledons and leaves of young *B. napus* seedlings. After germination, *Lm* hyphae penetrate through the wounds and stomata, and, as infection progresses, hyphae continue to grow between the cells and into the stem, eventually causing lesions at the base of the stem (stem canker) (Fitt *et al.*, 2006; Rouxel *et al.*, 2011). Disease symptoms on the cotyledons and leaves of *Brassica* species are visible as the formation of chlorotic tissue surrounding the site of infection, which develops into lesions with pycnidia occurring as black dots on the surface. Blackleg is a challenging disease to study as it exhibits an extremely complex life cycle in the host plant. *Lm* starts its life cycle as a biotroph during infection of the cotyledons and leaves, as an endophyte whilst growing in the stem and, finally, as a necrotroph leading to the formation of canker (Rouxel and Balesdent, 2005; Rouxel *et al.*, 2011; West *et al.*, 2001). The resistance of *B. napus* to *Lm* at the cotyledon stage is race specific. To date, 16 cotyledon resistance (*R*) genes (*Rlm1–Rlm11*, *RlmS*, *LepR1–LepR4*) have been reported from *Brassica* species (Raman *et al.*, 2013). Two of these genes, *LepR3* and *Rlm2*, encoding receptor-like proteins (RLPs), have been cloned (Larkan *et al.*, 2013, 2015). Six *Lm* avirulence (effector) genes (*AvrLm1*, *AvrLm2*, *AvrLm4-7*, *AvrLm6*, *AvrLmJ1* and *AvrLm11*), corresponding to the above-named *R* genes, have been cloned (Balesdent *et al.*, 2013; Fudal *et al.*, 2007; Ghanbarnia *et al.*, 2015; Gout *et al.*, 2006; Parlange *et al.*, 2009; Van de Wouw *et al.*, 2014). The genome sequence of the *Lm* isolate v23.1.3 revealed that the majority of the known and predicted effectors are located within AT-rich isochores (Rouxel *et al.*, 2011; Van de Wouw *et al.*, 2014). Despite these advances, there has been no comprehensive study describing the regulation of plant defence responses and pathogen virulence genes during the foliar infection of *B. napus*.

Dual RNA-sequencing (RNA-seq) allows accurate gene expression analysis of plant pathogens and their respective hosts simultaneously, and has been applied to investigate biotrophic and necrotrophic fungal–host interactions (Metzker, 2010; Westermann *et al.*, 2012). The recent release of the *B. napus* cv. Darmor genome sequence (Chalhoub *et al.*, 2014) and the availability of a reference genome for *Lm* (Rouxel *et al.*, 2011) have provided the opportunity to investigate the molecular interaction in the *B. napus–Lm* pathosystem. To date, the only RNA-seq reported for the *B. napus–Lm* interaction is the study by Lowe *et al.* (2014). They compared the expression of *Lm* and *B. napus* genes at 7 and 14 days after inoculation (dai). Although limited in its scope (only two time points and a total of 164.9 million reads), this work provided a general view of the gene expression profile during the *Lm–B. napus* interaction (Lowe *et al.*, 2014). These authors, as well as Šašek *et al.* (2012), reported the up-regulation of the plant hormones salicylic acid (SA) and ethylene (ET) in *B. napus* in response to *Lm* infection. Diverse plant hormones play a central role in the regulation of plant immune responses (Katagiri and Tsuda, 2010; Pieterse *et al.*, 2012). The roles of the plant hormones SA, jasmonic acid (JA) and ET in plant defence have been studied extensively. SA has a major role in resistance against biotrophic pathogens, whereas JA and ET regulate plant defence against necrotrophs (Glazebrook, 2005). Other hormones, such as abscisic acid (ABA), gibberellins (GAs), auxins, cytokinins (CKs), brassinosteroids (BRs) and nitric oxide (NO), have also been reported to function as modulators of the plant immune response (Pieterse *et al.*, 2012).

To obtain a comprehensive gene expression profile for both the pathogen and host during a compatible interaction between *B. napus* and *Lm*, RNA prepared from the cotyledon tissues of the susceptible *B. napus* cv. Topas at 0, 2, 4, 6 and 8 dai was sequenced. In total, 1.38 billion reads for four biological replicates were generated using the Illumina HiSeq-2500 platform. These data enabled us to define the lifestyle transition of *Lm* and to reveal the regulation of *B. napus* defence genes during cotyledon infection. In addition, we present the expression profile of known and candidate *Lm* effector genes during infection and provide evidence that supports the virulence function of some of the predicted effectors.

RESULTS

Disease progression on *B. napus* seedlings

One-week-old cotyledons of the doubled-haploid (DH) line *B. napus* cv. Topas DH16516 were inoculated with pycnidiospores of *Lm* isolate 00-100. Under our inoculation protocol, infection initiated by the pycnidiospores continued without any visible symptoms for the first 3–4 dai. At 4 dai, a chlorotic ring surrounding the inoculation site became clearly visible, which later (8 dai)

expanded, leading to the formation of a lesion and to tissue collapse around the site of inoculation (Fig. 1A). RNA was prepared from the cotyledon discs surrounding the site of inoculation, sampled at 0, 2, 4, 6 and 8 dai.

RNA-sequencing

We applied the dual deep RNA-seq approach to simultaneously assess genome-wide expression profiling of *B. napus* and *Lm* at five different time points. For each time point, 28.7–115.6 million paired-end reads were produced and a total of 1.38 billion RNA-Seq reads were generated for four biological replicates (Table S1, see Supporting Information). In addition, 15.4 million paired-end RNA-seq reads were generated from an *in vitro*-grown *Lm* culture. Based on the count distribution, density plots (Fig. S1A, see Supporting Information), clustering of the sample-to-sample distances (Fig. S1B) and the MA-plot (Fig. S1C), the best three of four RNA-seq replicates were chosen for gene expression analysis. All reads were mapped to the genome sequence of *Lm* isolate v23.1.3 and the *B. napus* cv. Darmor reference genome (Chalhoub *et al.*, 2014; Rouxel *et al.*, 2011). The percentages of reads, for each time course, mapped to the pathogen and host genomes are indicated in Fig. 1 and Table S1.

Differentially expressed genes (DEGs) were detected using the DESeq2 package. Genes with a false discovery rate-Benjamini–Hochberg (FDR-BH) of less than 0.05 were considered to be differentially expressed. Variability among the samples was determined by preparing a clustering image map (CIM) of the sample-to-sample distance matrix and principal component analysis (PCA). The PCA and CIM analysis displayed a clear distinction in the transcriptome of *Lm* at different time points (Fig. 1B,C).

Lm gene expression profile during infection

The expression profile of 12,469 *Lm* predicted genes showed that close to 74% of the *Lm* genes were expressed during the *B. napus* infection [reads per kilobase of exon per million mapped reads (RPKM) > 2] and 56% were expressed during *Lm in vitro* growth. A total of 2898 genes showed differential expression (FDR-BH < 0.05) in at least one time point, with 621 only expressed during host infection (no expression during *in vitro* growth) (Fig. 1D). Genes with significant changes in expression were determined by pair-wise comparison of the infection time course (i.e. 2 vs. 0 dai, 4 vs. 2 dai, 6 vs. 4 dai, 8 vs. 6 dai). The total numbers of DEGs for each of these comparisons were 40, 163, 384 and 2692, respectively. A major portion (40%) of the DEGs at the earlier time points during infection (2 vs. 0 dai) included the predicted secreted protein-encoding genes (SPs), which, in addition to effectors (SP) of unknown function, consisted of the plant cell wall-degrading enzymes (PCWDEs). The most prevalent PCWDEs at this early stage of infection were the pectin-degrading enzymes, such as glycoside hydrolase (GH) family 28, GH105 and several
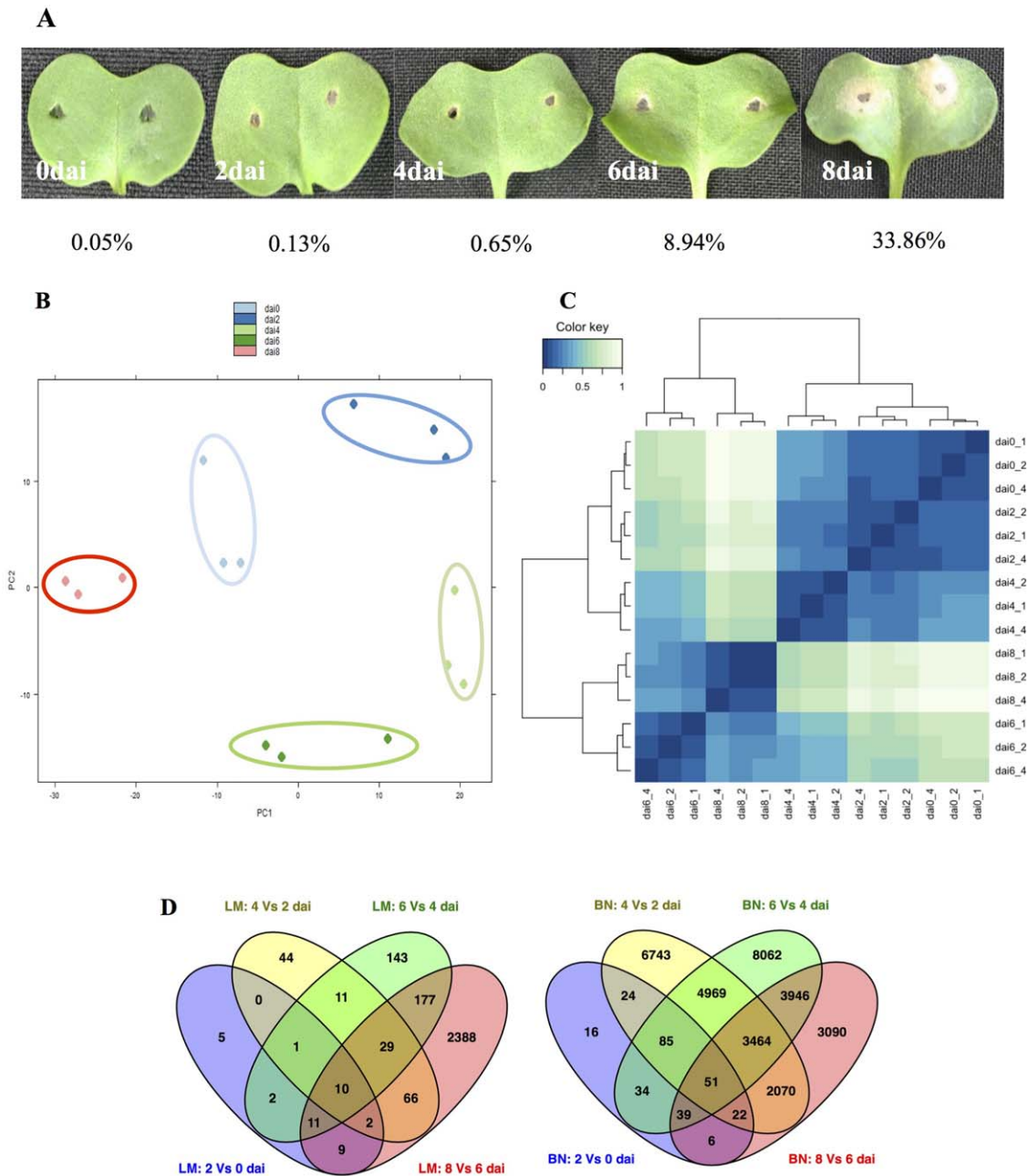
Fig. 1 Disease symptoms on cotyledons of the susceptible *Brassica napus* cv. DH-Topas 16516 (DHT) infected with *Leptosphaeria maculans* isolate 00-100. (A) Cotyledons were photographed at 0, 2, 4, 6 and 8 days after inoculation (dai). The percentages of reads aligned to the genome of *L. maculans* isolate v23.1.3 for each time point are presented. (B, C) Global evaluation of RNA-sequencing in *L. maculans*. Principal component analysis (PCA) (B) and clustering image map (CIM) (C) display a clear distinction among the transcriptome of *L. maculans* at different time points. (D) Differentially expressed genes (DEGs) that are unique or shared among various time point comparisons in 00-100 (left, LM) and DHT (left, BN). The numbers of DEGs are noted in each section of the Venn diagrams.

pectate lyases (PL1, PL9, PL10, PL11). Pectin is the main component of the cell wall of dicots and, when depolymerized, the plant cell wall becomes more vulnerable and accessible to other PCWDEs (Malinovsky *et al.*, 2014). The *Lm* genes encoding for chitinases were highly expressed at 2 dai, which is consistent with

the role of these enzymes in the growth and development of fungi. The *Lm* pattern of gene expression at 4 dai was similar to that at 2 dai, with 25% of the total DEGs annotated as potential effectors. In addition to GH and PL classes of Carbohdrate-Active enZYmes (CAZy), several genes containing carbohydrate-binding

modules (CBMs), including CBM50, which binds chitin (LysM domain-containing proteins), were differentially expressed at 2 and 4 dai. The expression profiles of *Lm* genes during the first 4 days of *Brassica* infection support an initial biotrophic establishment of *Lm*, which was evident by the relative abundance of effectors (secreted by the pathogen to suppress plant defence) and the reduced number of PCWDEs (largely consisting of pectinases). However, the pattern of DEGs at 6 and 8 dai was more suited to a necrotrophic lifestyle. At these latter time points, predicted secreted proteins constituted a small portion of the total DEGs (15% at 6 dai and 6.9% at 8 dai) and CAZy-encoding genes at 6 and 8 dai were more abundant and diverse. A notable change in the CAZy profile at 6 and 8 dai was the expansion of GHs and CAZy belonging to the auxiliary activities (AA) group. AAs help GH gain access to the carbohydrates embedded in the plant cell wall (Levasseur *et al.*, 2013).

Other genes that were differentially expressed during infection were genes related to nucleotide and amino acid biosynthesis, starch and sucrose metabolism, nucleotide and amino acid sugar metabolism, and sugar and other transporter families. Differential expression of transporter genes was observed as early as 2 dai and a major facilitator superfamily (MFS) of sugar transporters was highly expressed at this time point. Among the predicted transporter genes with significant changes in expression level, sugar/carbohydrate transporters were prevalent at 4, 6 and 8 dai. There was a significant increase in the numbers and types of transporter genes differentially expressed at 8 dai (amino acid and metal ion transporters) coinciding with the lysis of the host plant tissues and the release of nutrients, as well as toxins and antimicrobial compounds, at this stage.

A search for the genes involved in the biosynthesis of secondary metabolites identified 25 core genes, including polyketide synthases (PKSs), non-ribosomal peptide synthetases (NRPSs) and dimethylallyltryptophan synthetase/CymD prenyl transferase (DMATS) (Fig. S2, see Supporting Information). Fungal secondary metabolites have diverse functions, including their role as virulence factors in necrotrophic fungi through the production of toxins (Cho, 2015). Using the software SMURF (Khaldi *et al.*, 2010), we predicted 14 PKSs for *Lm*. The expression of *Lm* secondary metabolite genes was increased at 6 dai and the majority were highly up-regulated at 8 dai, which coincides with the necrotrophic stages of *Lm* during *B. napus* cotyledon infection. Our results showed significant up-regulation of *PKS6*, *PKS10*, *PKS13* and *PKS14* at 8 dai, but no transcript was detected for *PK2*, *PK4*, *PK8*, *PK11* and *PK12* (Fig. S2). *Lm* PKS10 shows 92% similarity to PKS responsible for the biosynthesis of melanin, a secondary metabolite that contributes to fungal structures and has been reported to play a role in the pathogenicity of human and plant fungi (Elliott *et al.*, 2013; Jacobson, 2000; Scharf *et al.*, 2014). PKS13 and PKS14 have been reported to be required for the production

of phomenoic acid, an *Lm* metabolite that is toxic towards *L. biglobosa*, another pathogen of *B. napus*. It has been suggested that the production of phomenoic acid helps *Lm* to outcompete other fungi in its environmental niche (Elliott *et al.*, 2013). *Lm* PKS6 has been reported to have an unusual structure by containing both a reductase and a methyl transferase domain not reported previously (Elliott *et al.*, 2013). The expression of the *Cladosporium fulvum* PKS6 gene has been reported to be reduced during the initial stages of fungal growth, but elevated during the later stages of infection, when conidiophores emerge from the infected plants (Collemare *et al.*, 2014). Another class of enzyme involved in the production of secondary metabolites is the NRPSs. *Lm* NPRSs have been reported to be involved in the production of the non-host-selective phytotoxin, sirodesmin PL. *Lm* lines with a mutation in an *Lm* NPRS gene named 'SirP' were less virulent during the colonization of *B. napus* stem, but not cotyledon (Elliotte *et al.*, 2007). We searched the *Lm* predicted proteins to identify SirP homologues. SirP (jgi.p|Lepmu|2880) was not expressed during any time course in our experiment. Elliotte *et al.* (2007) detected the expression of this gene in infected cotyledons starting at 10 dai. We also found four genes (jgi.p|Lepmu|1264, jgi.p|Lepmu|1265, jgi.p|Lepmu|1295 and jgi.p|Lepmu|904) that encoded for proteins with significant homology (BLASTP; E value = 8E-90, 8E-51, 3E-93, 6E-105) to SirP. All of these four genes encoding for NRPs were differentially expressed during cotyledon infection (Fig. S2); however, their roles in the pathogenicity of *Lm* have not yet been established.

Defining *Lm* effectors

All of the *Lm* effectors identified to date are located within the AT-rich isochores of the genome (Rouxel *et al.*, 2011; Van de Wouw *et al.*, 2014), with the exception of *AvrLm2*, which resides in a GC island within the AT-rich region of the *AvrLm1-2-6* cluster (Ghanbarnia *et al.*, 2015). Rouxel *et al.* (2011) identified 122 predicted effectors to be located within the AT-rich blocks of the *Lm* genome.

To search for the *Lm* candidate effectors, we adopted the pipeline (Fig. 2A) that shares common features with the effector predication pipelines described for the filamentous plant pathogens (Guyon *et al.*, 2014; Pedersen *et al.*, 2012; Sperschneider *et al.*, 2015). In total, 668 SPs, 310 of which were small (<300 amino acid) secreted proteins (SSPs), were identified. Included within the SSPs were all the previously cloned *AvrLm* genes, except for *AvrLm1*, which was absent from our list of predicted effectors because of the deletion of the 43-bp N-terminal fragment (expanding the signal peptide) for the predicted AvrLm1 protein (jgi.p|Lepmu1|10780, Lema_P049660.1; accession number: XM_00385577). Of the 668 SPs, 162 genes had no detectable transcript during infection and 210 genes showed differential expression (Fig. 2B), with 80 being SSPs (Fig. 2C, Table S2, see
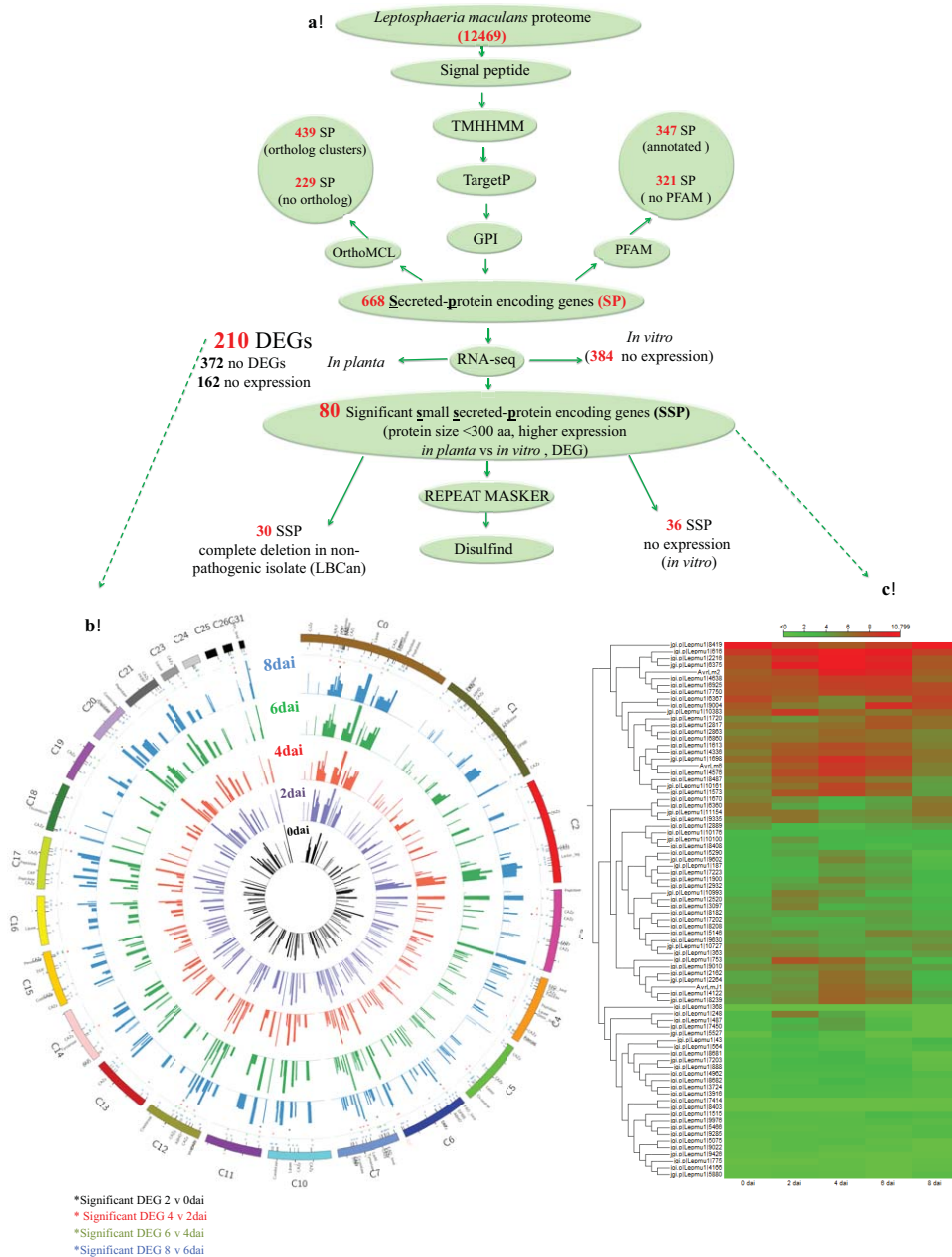
Fig. 2 *Leptosphaeria maculans* (*Lm*) secretome prediction pipeline. (A) Features used to predict and classify effectors of *Lm*. aa, amino acid; DEG, differentially expressed gene; GPI, Glycophosphatidylinositol-anchor; RNA-seq, RNA-sequencing; (B) *Lm* genes encoding predicted secreted proteins (SPs) and their expression levels during different time points. The outermost ring shows 210 of 668 SPs in the *Lm* genome that were differentially expressed in at least one time point comparison. Circles (from inside to outside) represent the expression of each gene at 0 (black), 2 (purple), 4 (red), 6 (green) and 8 (blue) days after inoculation (dai). Known effectors *AvrLm2*, *AvrLm6* and *AvrLmJ1*, located on supercontigs 6 and 7 of *Lm* v23.1.3, are highlighted in red. (C) Heat map of the 80 predicted small secreted protein (SSP)-encoding genes differentially expressed during infection at different time points. The expression of each gene is based on regularized logarithmic transformation of the average of the best three biological replicates using DESeq2. The Euclidean distance for the distance measure and average linkage for cluster linkage criteria were selected.

Supporting Information). These 80 SSPs were considered as the most likely set of *Lm* effectors. Within the 80 SSPs, expression of the known effector genes *AvrLm2*, *AvrLm6* and *AvrLmJ1* was up-regulated at 4 and 6 dai, and then reduced at 8 dai, confirming the previously reported pattern of expression for these genes (Ghanbarnia *et al.*, 2015). *AvrLm1* and *AvrLm11* were deleted and *AvrLm4-7* was not expressed in the *Lm* isolate 00-100 used in our study. One of the predicted SSPs (Lema_T086540.1) had

Table 1 A list of 16 highly expressed *Leptosphaeria maculans* predicted effectors selected for biological assay.

Pfam	Gene ID	Protein ID	Super contig	Start	End	Protein size	Cys*	DB†	Complete deletion in non-pathogenic isolate (*LBCan*)‡
–	jgi|Lepmu1|616	Lema_T006160.1	0	2286679	2287371	213	6	3	Yes
–	jgi|Lepmu1|7450	Lema_T023440.1	2	76723	77286	121	3	0	Yes
–	jgi|Lepmu1|8487	Lema_T033060.1	3	287921	288676	123	8	4	Yes
–	jgi|Lepmu1|8681	Lema_T035000.1	3	1031016	1031559	124	7	2	Yes
–	jgi|Lepmu1|9004	Lema_T038230.1	3	2336898	2337410	114	6	3	
–	jgi|Lepmu1|9010	Lema_T038290.1	4	69859	70849	291	12	>5	Yes
–	jgi|Lepmu1|1613	Lema_T076380.1	10	1509440	1509941	96	6	3	Yes
–	jgi|Lepmu1|1698	Lema_T086540.1	11	92980	93502	121	7	3	Yes
–	jgi|Lepmu1|2162	Lema_T083940.1	12	646590	646977	129	7	3	Yes
–	jgi|Lepmu1|2216	Lema_T084480.1	12	827862	828642	187	6	3	Yes
–	jgi|Lepmu1|2264	Lema_T084960.1	12	946778	947374	144	5	2	
–	jgi|Lepmu1|2817	Lema_T081180.1	13	1193860	1194346	104	5	2	Yes
–	jgi|Lepmu1|2863	Lema_T081640.1	13	1352945	1353440	91	9	4	Yes
–	jgi|Lepmu1|3097	Lema_T095640.1	14	681916	682620	178	10	>5	
CAP	jgi|Lepmu1|4336	Lema_T100080.1	17	427889	428585	232	5	0	
–	jgi|Lepmu1|6375	Lema_T113200.1	20	228261	228840	193	5	1	

*Cysteine residues.

†DISULFIND (Ceroni *et al.*, 2006) was also used to predict the disulfide bonding (DB) state of cysteines and their disulfide connectivity.

‡Unpublished data.

homology (42% identity) to Six5, an effector from *Fusarium oxysporum* reported by Ma *et al.* (2015). Lema_T086540.1 was significantly up-regulated at 2 and 4 dai but was not expressed during *in vitro* growth (Fig. S3A, B, see Supporting Information). Sequence alignment revealed the presence of six cysteines that were conserved between Lema_T086540.1 and Six5 (Fig. S3C).

Sixteen of the 80 SSPs that showed very low variance among the biological replicates and were highly expressed during infection (Table 1) were selected for transient assay in *Nicotiana benthamiana*. Four of these SSPs partially or fully suppressed cell death induced by the mouse pro-apoptotic Bax gene, when co-expressed in *N. benthamiana* (Fig. 3A).

The necrosis and ET-inducing peptide-1 (Nep-1)-like protein (NLP) (Gijzen and Nürnberger, 2006) was also differentially expressed. NLP expression in hemibiotrophic fungi coincides with the initiation of the necrotrophic phase (Qutob *et al.*, 2002; Zaparoli *et al.*, 2011). Expression of *Lm* NLP (*Lm-NLP*) was first detected at 4 dai, increased at 6 dai and remained at the same level at 8 dai (Fig. 3B). This expression pattern provides further evidence for the biotrophic lifestyle of *Lm* within the first 4 days of cotyledon infection fallowed by a shit to necrotrophism. *Lm-NLP* function was confirmed by its ability to cause hypersensitive response (HR)-like cell death when transiently expressed in *N. benthamiana* leaves (Fig. 3C). To further determine the role of NLP during *Lm* infection, we generated transgenic *Lm* lines expressing an NLP-RNAi construct. Twenty NLP-RNAi transformants (Lm-nlp) were selected and their virulence was examined by inoculation on cotyledons of the susceptible *B. napus* cv. Topas DH16516. As shown in Fig. 3D, three of the Lm-nlp lines (NLP-SL1, NLP-SL2 and NLP-SL3) were severely compromised in viru-

lence. Reduction in *NLP* expression was confirmed by quantitative polymerase chain reaction (qPCR) (Fig. S4A, see Supporting Information). In comparison with wild-type *Lm*, Lm-nlp lines showed a slightly reduced growth rate, but sporulated normally on culture plates (Fig. S4B).

Regulation of plant hormones and defence in *B. napus* infected by *Lm*

To define the *B. napus* hormone defence networks in response to *Lm* infection, we used HORMONOMETER software (Volodarsky *et al.*, 2009) which compares the input query genes against a database of Arabidopsis genes expressed in response to the application of different hormones. Using the Arabidopsis orthologues of the *B. napus* DEG as query, we obtained profiles of hormone regulation in *B. napus* at different time points after infection (Fig. 4A). This comparison revealed a correlation of the *B. napus* response at the initial phase of infection (2–4 dai) with the gene expression response of Arabidopsis treated with SA, whereas, at the later stages of infection (6 and 8 dai), there was a good correlation with the Arabidopsis gene expression profile in response to the application of JA. Analysis by the software MapMan (Thimm *et al.*, 2004) also showed that upstream genes of the JA pathway were up-regulated in *B. napus* at 6–8 dai (Fig. 4B). There was a good correlation throughout all time points with the Arabidopsis genes related to ET. In the case of ABA signalling, the *B. napus* response at 4 dai correlated with the Arabidopsis response to ABA. Taken together, these data underline the importance of SA, ET and JA pathways, and provide evidence for the involvement of
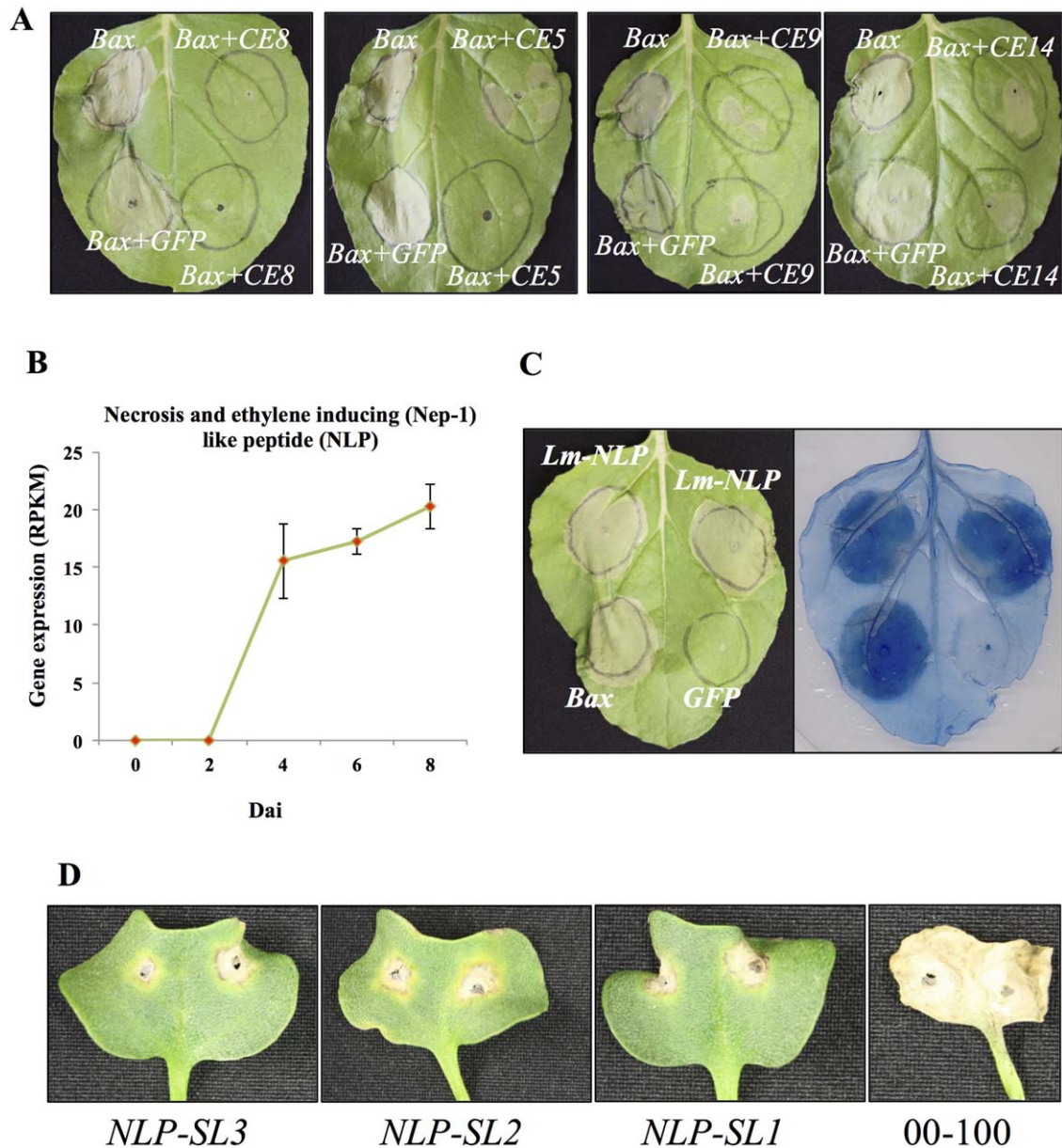
Fig. 3 Suppression of BAX-induced cell death (CD) by *Leptosphaeria maculans* candidate effectors in *Nicotiana benthamiana* (*Nb*) leaves. *Agrobacterium tumefaciens* (*Ag*) strains expressing individual *L. maculans* small secreted proteins (SSPs) and Bax were infiltrated into *Nb* leaves. *Ag* carrying pGWB451-GFP was used as a negative control. BAX-induced cell death was scored at 4 days after infiltration. (A) Examples of complete suppression of CD by CE8 (jgi|Lepmu1|2216; Lema_T084480.1) and partial suppression of CD by CE5 (jgi|Lepmu1|4336; Lema_T100080.1), CE9 (jgi|Lepmu1|616; Lema_T006160.1) and CE14 (jgi|Lepmu1|9004; Lema_T038230.1) effectors. (B–D) *Leptosphaeria maculans* necrosis and ethylene-inducing peptide-1 (Nep-1)-like protein (NLP) (*Lm-NLP*) are required for the complete virulence of *Lm*. (B) Expression of *Lm-NLP* at different time points. (C) Transient expression of *Lm-NLP* in *Nb* leaves induces hypersensitive response (HR)-like cell death. *Nb* leaves were infiltrated with *Ag* cultures containing *Lm-NLP*, *Bax* and green fluorescent protein (*GFP*). *Bax* and *GFP* served as positive and negative controls, respectively. Leaves were photographed 5 days after infiltration (left panel) and cell death was visualized by trypan blue staining of the same leaves (right panel). (D) Cotyledons of 7-day-old seedlings of *Brassica napus* cv. DH-Topas 16516 were inoculated with the *L. maculans* wild-type isolate 00-100 and the three *Lm-NLP* silenced (RNAi) lines (*NLP-SL1*, *NLP-SL2* and *NLP-SL3*), and were photographed at 14 days after inoculation.

ABA in *B. napus* in response to *Lm* infection. Furthermore, the induction of SA in *B. napus* at 2 and 4 dai substantiates the biotrophic phase of *Lm* described above.

The profile of the *B. napus* DEGs showed multifaceted defence responses that peaked at 4 dai. The pattern recognition receptors CERK1 (chitin elicitor receptor kinase 1), extracellular RLPs,
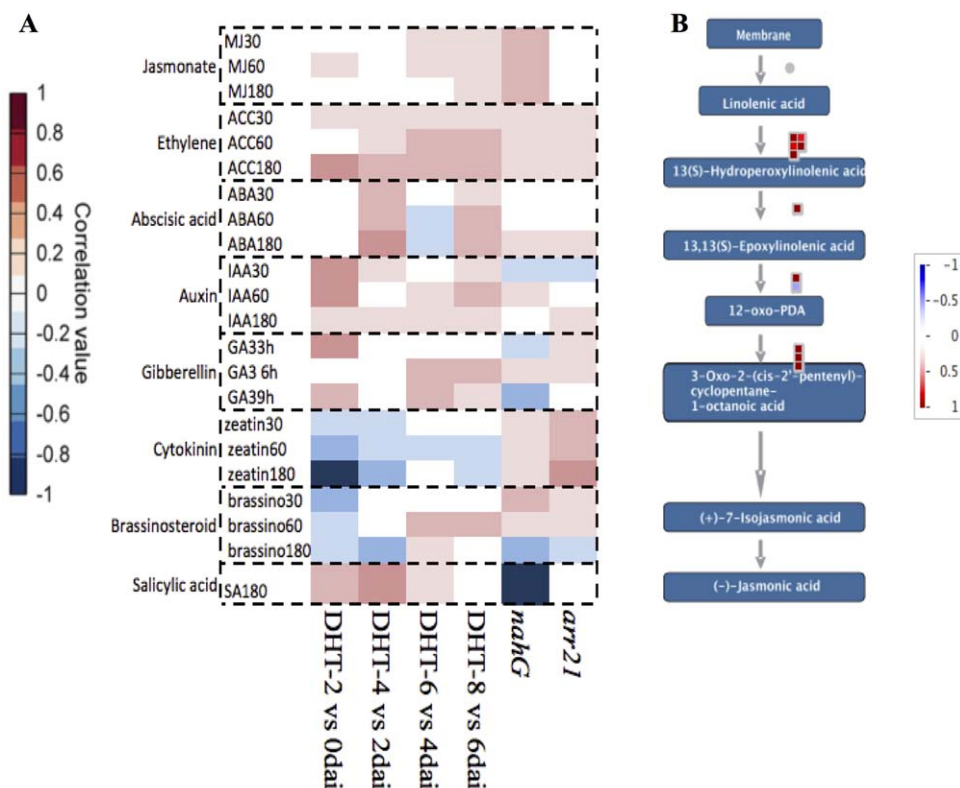
Fig. 4 *Brassica napus* hormonal response to *Leptosphaeria maculans* infection. (A) A positive correlation between the query (*B. napus* differentially expressed genes) and the *Arabidopsis thaliana* genes expressed when treated with various plant hormones is denoted in red, whereas a negative correlation is represented by blue. The transcriptomes of the Arabidopsis mutants *arr2*1 and *nahg* with increased cytokinin and decreased salicylic acid responses, respectively, are also included. (B) Jasmonic acid (JA) signalling pathway. MapMan output of JA-related genes that were differentially expressed at 8 vs. 6 days after inoculation (dai) ($\geq$log two-fold change). Each square represents one gene. Intensity scale: red represents up-regulated and blue represents down-regulated genes.

receptor-like kinases (RLKs) and wall-associated kinases (WAKs) were among the differentially expressed cell surface receptors that probably perceive *Lm* PAMPs (pathogen-associated molecular patterns) and effectors. It has been shown previously that the *Arabidopsis thaliana* LRR-receptor-like kinase (LRR-RLK) suppressor of Bir-1 (AtSOBIR1) interacts with LRR-RLP resistance genes (Liebrand *et al.*, 2014). We have also reported recently that AtSOBIR1 interacts with the *B. napus* Rlm2 (Larkan *et al.*, 2015). The expression of five of the six copies of *B. napus* SOBIR1 homologues peaked at 6 and 8 dai (Fig. S5, see Supporting Information).

Other genes with reported function in plant defence that were differentially expressed included genes encoding for proteases and protease inhibitors, chitinases, peroxidases, transcription factors (WRKY, AP2/EREBP, MYB), genes related to the production of the secondary metabolites and genes involved in plant cell wall reinforcement. The majority of these genes were down-regulated in the lesion zone surrounding the inoculation site (samples taken at 6 and 8 dai). Among the differentially expressed WRKY transcription factors with a proven role in plant defence were WRKYs 33, 40 and 51.

Lignification of the plant cell wall blocks pathogen entry at the site of infection and is triggered in response to pathogen infection.

As depicted in Fig. 5, the expression of the majority of the genes involved at the early steps of lignin biosynthesis [phenylalanine ammonia lyase (PAL), cinnamate 4-hydroxylase (C4H), 4-coumarate:CoA ligase (4CL)] increased at 4 dai and remained up-regulated at 6 and 8 dai.

Glucosinolates (GLSs) are sulfur- and nitrogen-containing secondary metabolites found in members of Brassicaceae. The role of GLSs in plant immunity, particularly against necrotrophic plant pathogens, has been well studied (Buxdorf *et al.*, 2013; Laluk and Mengiste, 2010). We found three GLS-related genes that were significantly up-regulated at 6 and 8 dai. Two of these genes, the cytochrome P450 (CYP79B2) and SUPERROOT1 (SUR1), are part of the GLS biosynthesis pathway (Fig. S6, see Supporting Information). The expression of another GLS-related gene, nitrile-specifier protein 5 (NSP5), was highly up-regulated at 4 dai and its expression continued to increase at 6 and 8 dai.

DISCUSSION

The genetics of cotyledon resistance to *Lm* have been studied in detail; however, the genomic research of the *B. napus*–*Lm*
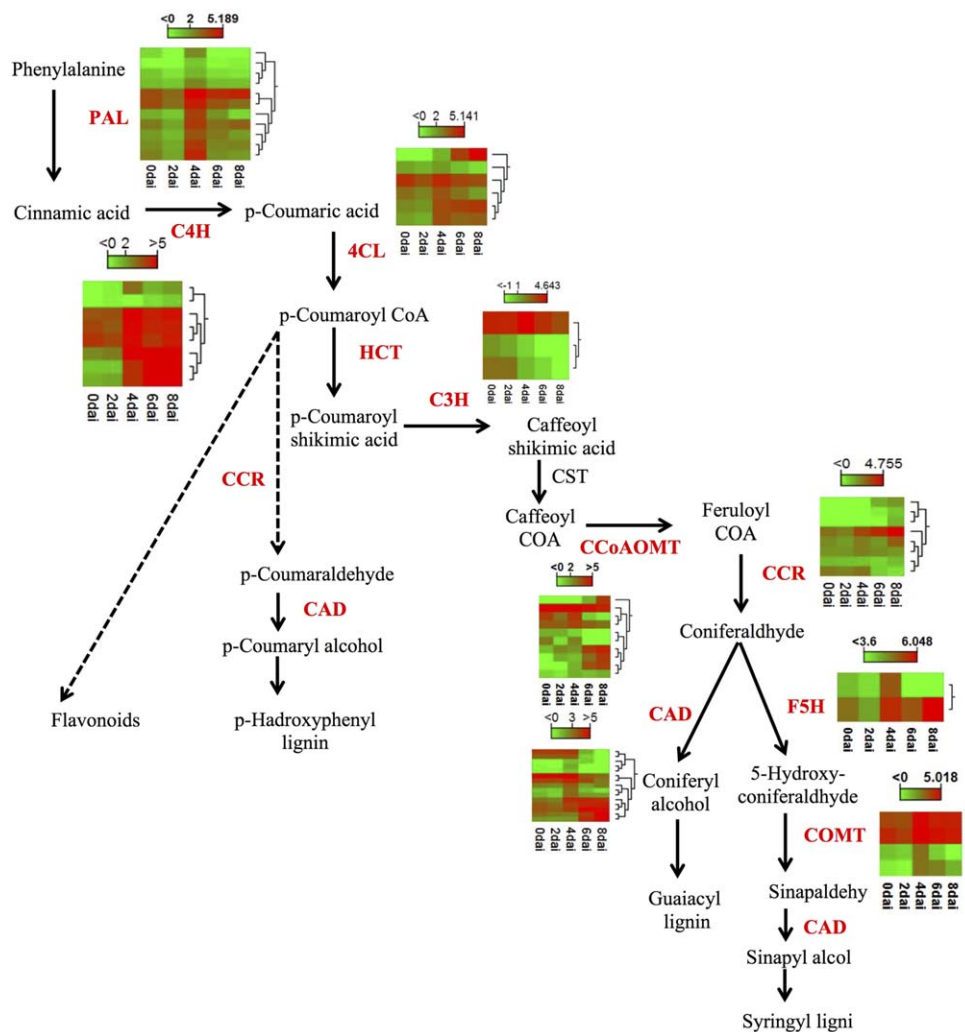
Fig. 5 Expression profile of *Brassica napus* lignin-related genes at different time points in response to *Leptosphaeria maculans* infection. Heat map presents the expression of genes ranging from green (low) to red (high). CAD, cinnamyl-alcohol dehydrogenase; CCoA-3H, cinnamyl-alcohol dehydrogenase; CCoAOMT, caffeoyl-CoA *O*-methyltransferase; CCR, cinnamoyl-CoA reductase; C3H, *p*-coumarate 3-hydroxylase; C4H, cinnamate 4-hydroxylase; 4CL, 4-coumarate:CoA ligase; COMT, caffeic acid *O*-methyltransferase; CST, p-hydroxycinnamoyltransferase; F5H, ferulate 5-hydroxylase; HCT, p-hydroxycinnamoyl-CoA; PAL, phenylalanine ammonia lyase.

interaction lags behind. Šašek *et al.* (2012) examined the expression of several marker genes, associated with various plant hormones, in resistant and susceptible *B. napus* plants infected with *Lm*, and reported that the expression of SA-related genes was induced at the earlier (4–6 dai) stages of *B. napus* infection, whereas the expression of the genes related to the ET pathway increased at the later stages (8–10 dai). Similarly, Lowe *et al.* (2014) have reported recently that the marker genes for SA and ABA were up-regulated at 7 and 14 days after infection of *B. napus* with *Lm*, respectively.

Here, we provide a more detailed picture of the global transcriptome that is active in *B. napus* and *Lm* during cotyledon infection. The expression profile of the genes related to different plant hormones revealed the importance of SA at the earlier stages of infection (until 4 dai) and the up-regulation of genes related to the JA pathway at the later stages (6–8 dai) (Figs 5 and 6). Consistent with this, Šašek *et al.* (2012) reported that the application of benzothiadiazole (BTH), a functional analogue of SA, provided full immunity against *Lm* infection in *B. napus*. These authors reported similar results when *B. napus* was treated with the ET precursor 1-aminocyclopropane-1-carboxylic acid (ACC) or ABA; however, BTH had a much stronger effect than ACC and ABA in preventing *Lm* infection.

Recent large-scale transcriptomic and genomic studies have revealed the importance of other plant hormones, such as auxin, BRs, GAs and CKs, in plant defence (Robert-Seilaniantz *et al.*, 2011). The analysis of the expression of plant hormone-related genes showed that, at 6–8 dai, *B. napus* genes related to the BR pathway showed a positive correlation with the gene expression profile of Arabidopsis in response to BR (Fig. 5). The role of BRs in *B. napus* defence against *Lm* becomes more significant in the light of recent studies revealing the involvement of BRs in PAMP-triggered immunity (PTI) (Albrecht *et al.*, 2012), and the striking overlap that exists between the PAMP recognition complexes and the plant receptor complexes for the recognition of intercellular filamentous pathogens (Liebrand *et al.*, 2014). Several recent
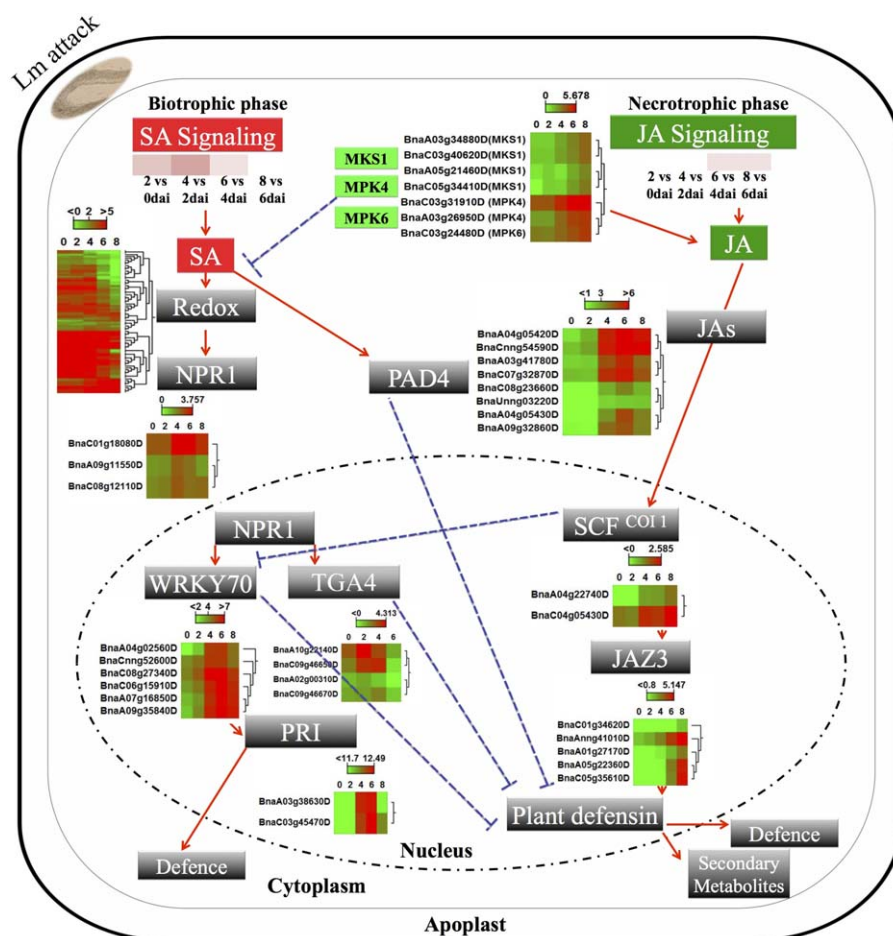
Fig. 6 An overview of salicylic acid (SA) and jasmonic acid (JA) signalling in *Brassica napus* in response to infection with *Leptosphaeria maculans*. The expression profiles of *B. napus* genes with homology to known marker genes related to SA and JA pathways are presented as green (low) or red (high). MKS1, MAP kinase substrate 1; MPK4, mitogen-activated protein kinase 4; MPK6, mitogen-activated protein kinase 6; SA, salicylic acid; JA, jasmonic acid; NPR1, natriuretic peptide receptor 1; WRKY70, wall-associated receptor kinase; PR1, pathogenesis-related protein 1.

studies have shown that SOBIR1 and BAK1 (BRI1-associated kinase 1) form a complex with tomato RLPs to recognize *C. fulvum*, the pathogen of tomato (Postma *et al.*, 2015). *Lm* shares a high degree of similarity with *C. fulvum*, in term of its infection process and host plant receptor complex. We have reported recently that a similar mechanism exists for the perception of *Lm* by *B. napus* (Larkan *et al.*, 2015, Ma and Borhan, 2015). BAK1 is a co-receptor for BR and PAMP. In a recent paper, Belkhadir *et al.* (2012) reported that increased BR signalling antagonizes BAK1-mediated cell death. It is conceivable that BRs contribute to *B. napus* defence against *Lm* in a similar manner as described for PTI (Wang, 2012). Interestingly, BR signalling in response to *Lm* infection in our experiment was down-regulated at the initial stage of infection that coincides with the activation of RLP-RLK receptor complexes, but genes related to the BR pathway were up-regulated once the lesion had developed (6–8 dai). The up-regulation of BR-related genes at the necrotrophic stage of *Lm* growth could, at least in part, be a result of the production of toxins by *Lm* at the late stages of infection. Phytotoxins produced by *Fusarium* strains have been reported to induce BRs (Masuda *et al.*, 2007).

As it is an intercellular pathogen, plant cell surface receptors play a primary role in the initiation of *B. napus* defence against *Lm* (Stotz *et al.*, 2014; Larkan *et al.*, 2013, 2015; Ma and Borhan, 2015). Several *B. napus* receptors were up-regulated in response to *Lm*, such as SOBIR1, RLKs containing DUF26 (domain of unknown function26), LRR-RKs (leucine-rich repeat receptor kinases) and WAKs. As reported previously, SOBIR1 is a part of the LRR-RLP recognition complex against *Lm* (Larkan *et al.*, 2015). DUF26 genes, also known as CRKs (cysteine-rich receptor kinases), are transcriptionally induced in response to pathogen and SA (Acharya *et al.*, 2007; Kim *et al.*, 2004; Wang *et al.*, 2013, 2014; Wrzaczek *et al.*, 2010). DUF26 transcripts were found to be abundant in the rice apoplast during *Magnaporthe oryzae* infection (Wang *et al.*, 2014). Overexpression of WAK in Arabidopsis and rice enhances resistance to *Botrytis cinerea* and *M. oryzae*, respectively (Wang *et al.*, 2014). We found many transcription factors, including some of the WRKY-type transcription factors, to be up-regulated in response to *Lm*. Several WRKYs have been reported to act as positive and negative regulators of plant defence (Peng *et al.*, 2008; Qiu *et al.*, 2008; Shimono *et al.*, 2007; Wang *et al.*, 2007; Zhang *et al.*, 2008).

Lm is considered to be a hemibiotroph during the foliar infection stage, but no molecular evidence supporting and defining the biotrophic and necrotrophic stages of *Lm* infection has been provided. We presented several pieces of evidence that defined the hemibiotrophic growth stages of *Lm* during *B. napus* cotyledon infection. The biotrophic stage of *Lm* growth, during the cotyledon infection of *B. napus*, was marked by the *B. napus* SA response at 2 and 4 dai, as well as the up-regulation of the majority of the predicted and known effectors. Other clear evidence was the expression of *Lm-NLP*, which was first seen at 4 dai and was at a maximum at 6 and 8 dai. The role of NLP in the induction of necrosis (which is required for necrotrophic growth) was demonstrated by transient assay in tobacco. In addition, we showed that the suppression of *NLP* expression by RNAi compromised virulence (lesion formation) in *Lm*. NLP is conserved among prokaryotic and eukaryotic microorganisms and is a well-known marker for the initiation of necrotrophy in plant-pathogenic fungi. The production of toxins by fungal plant pathogens is related to the necrotrophic lifestyle. The expression of several of the *Lm* genes encoding PKSs and NRPSs, with a reported or potential role in the production of toxins in fungi, was upregulated at 6–8 dai (Fig. S2). Some of the *Lm* toxins, such as sirodesmin, have been reported to play a role in the virulence of *Lm* during infection of the *B. napus* stem; however, their role in the development of lesions during cotyledon infection is unclear. The expression of three *B. napus* genes (identified as CYP79B2, SUR1 and NPS5) related to GLSs was also up-regulated at the later stages (6–8 dai) of infection. GLSs, mainly found in members of Brassicaceae, are constitutively present in a non-reactive form, but, on tissue damage and pathogen attack, are hydrolysed, resulting in the production of physiologically active derivatives, such as isothiocyanates (ITCs), thiocyanates and simple nitriles. The role of GLSs in defence against several necrotrophic fungi has been reported (Buxdorf *et al.*, 2013; Stotz *et al.*, 2011). The Arabidopsis CYP79B2/B3 double mutant is more sensitive to the necrotrophic pathogens *Alternaria brassicicola* and *Botrytis cinerea* (Buxdorf *et al.*, 2013). SUR1 functions as a C-S lyase in the GLS pathway, and the Arabidopsis sur1 mutants are impaired in the production of GLSs (Mikkelsen *et al.*, 2004). NPSs, in association with myrosinase, are involved in the hydrolysis of GLSs and the formation of simple nitriles, a toxin with reported function against herbivores (Mumm *et al.*, 2008).

The RNA-seq conducted in this study allowed us to define a list that includes the most likely *Lm* effector genes, and the functions of several of these effectors in pathogen virulence and suppression of plant defence were confirmed. Future research on these effector genes should help to identify additional *Avr* genes and provide insights into the virulence mechanisms of *Lm*.

Canola breeders have exploited the *B. napus* resistance against *Lm* as the most effective and practical approach to control blackleg. Insights into the molecular interaction of *B. napus* and *Lm* described here, and additional research, will provide the knowledge and tools required for the genetic improvement of *Brassica* resistance against blackleg disease.

EXPERIMENTAL PROCEDURES

Plant material and fungal isolate

The *B. napus* DH line Topas DH16516 and a single-spore culture of the *Lm* isolate 00-100, which possesses three known effectors (*AvrLm2*, *AvrLm6* and *AvrLmJ1*), were used in this study. *Brassica napus* cv. Topas has been tested extensively against an international collection of *Lm* isolates (over 100 isolates) in our laboratory and has been proven to lack race-specific resistance against blackleg disease (Larkan *et al.*, 2013).

Plant growth and infection conditions

The plant growth and *Lm* infection conditions have been described previously (Larkan *et al.*, 2013). Plants were grown in a growth chamber at 20 °C, 16 h light, with a light intensity of *c.* 450 μmol/m^2/s at bench level, and 18 °C, 8 h dark. For pycnidiospore inoculation, a small wound was made in the centre of each cotyledon of 7-day-old seedlings and 10 μL of 2×10^7 spores/mL suspension were applied to each wound (four infection sites per seedling). After inoculation, the seedlings were kept under the same growth conditions and disease progression was monitored.

Total RNA isolation and library preparation for Illumina HiSeq 2500

The cotyledons of 7-day-old seedlings were inoculated with isolate 00-100. Mock inoculation with water served as a negative control. Cotyledon discs of 6 mm in diameter were excised from the infected cotyledons (four biological replicates) at 0, 2, 4, 6 and 8 dai. Twelve discs per sample were ground in liquid nitrogen, and then extracted with TRIzol LS reagent (Invitrogen, Carlsbad, USA) and purified by application to an Ambion mini RNA kit following the manufacturer's instructions. RNA was DNAase treated, quantified by a Qubit fluorometer (Invitrogen, Carlsbad, USA) and checked for quality by an Agilent Bioanalyzer 2100 (Agilent Technologies, Mississauga, Canada). Only samples with RNA integrity numbers above 8.0 were used for sequencing. Sequence reads (100 bp paired-end) were generated with Illumina TruSeq high-output version 3 chemistry on a HiSeq 2500 (Illumina, Inc., San Diego, USA) at NRC-Plant Biotechnology Institute (NRC-PBI), Saskatoon, SK, Canada.

Read mapping and gene expression analysis

In total, 1.38 billion raw reads were analysed in this study (Table S1). Reads were trimmed, adaptor sequences were removed and reads shorter than 15 bp were discarded (quality score limit, 0.05; trim ambiguous nucleotides <2) using CLC genomics workbench, version 7.5 (QIAGEN, Aarhus, Denmark). Trimmed sequences were mapped to the *B. napus* and *Lm* genomes using CLC genomics workbench (Mismatch cost = 2, Insertion cost = 1, Deletion cost = 1, Length fraction = 1, Similarity fraction = 0.97, Maximum number of hits allowed = 1). *Brassica napus* gene models were downloaded from the *Brassica napus* Genome

Resources – Genoscope and *Lm* gene models were obtained from the Joint Genome Institute (JGI) (http://genome.jgi.doe.gov/). Total reads per transcript and log$_2$ RPKM were obtained by the RNA-Seq Analysis function in CLC. The estimate SizeFactors and estimate Dispersions functions in the Bioconductor package DESeq2 v. 1.6.3 (Love *et al.*, 2014) were also used to normalize the raw transcript counts of *B. napus* and *Lm* genes, and to identify DEGs using the Benjamini–Hochberg (BH) method for correction of multiple comparisons. We also performed a CIM of the sample-to-sample distance matrix and PCA using *B. napus* and *Lm* genes to assess the variability among samples.

Functional classification based on Blast2Go and MapMan

Blast2Go-pro (Conesa and Gotz, 2008) software was used to annotate the DEGs. A Fisher's exact test was used to test the significance of gene ontology (GO) enrichment. KEGG (Kyoto Encyclopedia of Genes and Genomes; Kanehisa and Goto, 2000; Kanehisa *et al.*, 2014) enrichment analysis was performed using the KEGG function of Blast2Go-pro software to assign predicted pathways for DEGs. DEGs were analysed by MapMan software (Thimm *et al.*, 2004) using log two-fold changes in expression to visualize metabolic pathways and cellular responses of *B. napus* to *Lm*. PCWDEs were defined by conducting a similarity search of the CAZy database (db-CAN) (Yin *et al.*, 2012).

Hormonometer analysis

The putative *A. thaliana* orthologues of *B. napus* DEGs were imported to hormonometer software (Volodarsky *et al.*, 2009) to identify transcriptional similarities between DEGs and Arabidopsis genes related to different plant hormones.

Lm secretome prediction and analysis pipeline

We developed a pipeline to predict and classify effectors of *Lm*. We first detected the presence of an N-terminal signal peptide through signalP4.1 (Petersen *et al.*, 2011). Next, we excluded proteins with a predicted transmembrane domain as determined by TMHMM (Krogh *et al.*, 2001). Subsequently, we searched for the presence of subcellular localization signals using TargetP (Emanuelsson *et al.*, 2000). The presence of a glycosylphosphatidylinositol (GPI) anchor was predicted using PredGPI (Pierleoni *et al.*, 2008) to identify proteins anchored to the membrane. We used Pfam (Finn *et al.*, 2014) to verify biological functions enriched in the secretome of *Lm*. OrthoMCL (Fischer *et al.*, 2011) was used to identify homologous proteins based on sequence similarity by Markov clustering.

Vector constructions

To generate the RNAi constructs, the entire *Nep1* open reading frame (ORF) (GenBank accession LEMA_P070010.1) was amplified using the primer pair Nep-FB/Nep-RB. The PCR products were introduced into the entry vector pDON/Zeo (Life Technologies, Burlington, Canada) using the gateway protocol described by the manufacturer. For transient expression, pENTR/Zeo::*Nep1* was recombined into the binary vector pEarlyGate100 (Earley *et al.*, 2006). Genes for effector candidates were amplified from the *B. napus*–*Lm* cDNA library using the corresponding primer combina-

tions (Table S3, see Supporting Information) and recombined via the entry clone pDON/Zeo into the binary vector pGWB414 (Nakagawa *et al.*, 2007). Using the same approach, the mouse *Bax* gene was amplified with the primer pairs M-Bax-FB/M-Bax-RB (Table S3), cloned into pDON/Zeo and then recombined into the binary vector pEarlyGate100. All constructs were confirmed by sequencing. All resulting binary plasmids were transformed to the *Agrobacterium tumefaciens* strain GV3101 (pMP90).

RNAi-mediated silencing of *Lm*

The RNAi silencing plasmid pHGYGS::*Nlp1* was transformed into *A. tumefaciens* strain EHA105. *Agrobacterium*-mediated transformation of *Lm* isolate 00-100 was conducted based on the protocol described by Utermark and Karlovsky (2008). Quantitative PCR (qPCR) was performed as described previously (Ma and Borhan, 2015). qPCR primers are provided in Table S3.

Agrobacterium-mediated transient assay in *N. benthamiana*

Agrobacterium-mediated transient expression of candidate genes in *N. benthamiana* was performed according to the methods described previously (Ma *et al.*, 2012). Briefly, *Agrobacterium* was grown to an absorbance of 0.8 at an optical density at 600 nm (OD$_{600\ nm}$) in LB: Luria Broth–mannitol medium supplemented with 20 μM acetosyringone and 10 mM MES (2-(N-morpholino) ethanesulfonic acid) (pH 5.6). Cells were pelleted by centrifugation at 2500 g for 20 min and then re-suspended in infiltration medium (1 × MES; 10 mM MES, pH 5.6, 2% w/v sucrose, 200 μM acetosyringone). Leaves of 4–5-week-old *N. benthamiana* were infiltrated (OD$_{600}$ = 1) with a needleless syringe and photographed 3–5 days after infiltration. For the suppression of Bax-mediated cell death, the *A. tumefaciens*-containing *Bax* gene was infiltrated first and, 1 day later, the *A. tumefaciens* strain carrying the individual effector genes was infiltrated in the same spot. *Agrobacterium*-green fluorescent protein (GFP) served as the negative control. For light microscopy observation, leaves were boiled for 5 min in a 1 : 1 mixture of ethanol and 0.33 mg/mL trypan blue in lactophenol and destained overnight in 2.5 g/mL chloral hydrate solution.

REFERENCES

Acharya, B.R., Raina, S., Maqbool, S.B., Jagadeeswaran, G., Mosher, S.L., Appel, H.M., Schultz, J.C., Klessig, D.F. and Raina, R. (2007) Overexpression of CRK13, an Arabidopsis cysteine-rich receptor-like kinase, results in enhanced resistance to *Pseudomonas syringae*. *Plant J.* **50**, 488–499.

Albrecht, C., Boutrot, F., Segonzac, C., Schwessinger, B., Gimenez-Ibanez, S., Chinchilla, D., Rathjen, J.P., de Vries, S.C. and Zipfel, C. (2012) Brassinosteroids inhibit pathogen-associated molecular pattern-triggered immune signaling independent of the receptor kinase BAK1. *Proc. Natl. Acad. Sci. USA*, **109**, 303–308.

Balesdent, M.H., Fudal, I., Ollivier, B., Bally, P., Grandaubert, J., Eber, F., Chèvre, A.M., Leflon, M. and Rouxel, T. (2013) The dispensable chromosome of

Leptosphaeria maculans shelters an effector gene conferring avirulence towards *Brassica rapa*. *New Phytol.* **198**, 887–898.

Belkhadir, Y., Jaillais, Y., Epple, P., Balsemao-Pires, E., Dangl, J.L. and Chory, J. (2012) Brassinosteroids modulate the efficiency of plant immune responses to microbe-associated molecular patterns. *Proc. Natl. Acad. Sci. USA*, **109**, 297–302.

Buxdorf, K., Yaffe, H., Barda, O. and Levy, M. (2013) The effects of glucosinolates and their breakdown products on necrotrophic fungi. *PLoS One*, **8**, e70771.

Ceroni, A., Passerini, A., Vullo, A. and Frasconi, P. (2006) DISULFIND: a disulfide bonding state and cysteine connectivity prediction server. *Nucleic Acids Res.* **34**, W177–W181.

Chalhoub, B., Denoeud, F., Liu, S., Parkin, I.A., Tang, H., Wang, X., Chiquet, J., Belcram, H., Tong, C., Samans, B., Corréa, M., Da Silva, C., Just, J., Falentin, C., Koh, C.S., Le Clainche, I., Bernard, M., Bento, P., Noel, B., Labadie, K., Alberti, A., Charles, M., Arnaud, D., Guo, H., Daviaud, C., Alamery, S., Jabbari, K., Zhao, M., Edger, P.P., Chelaifa, H., Tack, D., Lassalle, G., Mestiri, I., Schnel, N., Le Paslier, M.C., Fan, G., Renault, V., Bayer, P.E., Golicz, A.A., Manoli, S., Lee, T.H., Thi, V.H., Chalabi, S., Hu, Q., Fan, C., Tollenaere, R., Lu, Y., Battail, C., Shen, J., Sidebottom, C.H., Wang, X., Canaguier, A., Chauveau, A., Bérard, A., Deniot, G., Guan, M., Liu, Z., Sun, F., Lim, Y.P., Lyons, E., Town, C.D., Bancroft, I., Wang, X., Meng, J., Ma, J., Pires, J.C., King, G.J., Brunel, D., Delourme, R., Renard, M., Aury, J.M., Adams, K.L., Batley, J., Snowdon, R.J., Tost, J., Edwards, D., Zhou, Y., Hua, W., Sharpe, A.G., Paterson, A.H., Guan, C. and Wincker, P. (2014) Plant genetics. Early allopolyploid evolution in the post-Neolithic *Brassica napus* oilseed genome. *Science*, **345**, 950–953.

Cho, Y. (2015) How the necrotrophic fungus *Alternaria brassicicola* kills plant cells remains an enigma. *Eukaryot. Cell*, **14**, 335–344.

Collemare, J., Griffiths, S., Iida, Y., Karimi Jashni, M., Battaglia, E., Cox, R.J. and de Wit, P.J.G.M. (2014) Secondary metabolism and biotrophic lifestyle in the tomato pathogen *Cladosporium fulvum*. *PLoS One*, **9**(1), e85877.

Conesa, A. and Gotz, S. (2008) Blast2GO: a comprehensive suite for functional analysis in plant genomics. *Int. J. Plant Genomics*, **2008**, doi:10.1155/2008/619832.

Earley, K.W., Haag, J.R., Pontes, O., Opper, K., Juehne, T., Song, K. and Pikaard, C.S. (2006) Gateway-compatible vectors for plant functional genomics and proteomics. *Plant J.* **45**, 616–629.

Elliott, C.E., Callahan, D.L., Schwenk, D., Nett, M., Hoffmeister, D. and Howlett, B.J. (2013) A gene cluster responsible for biosynthesis of phomenoic acid in the plant pathogenic fungus, *Leptosphaeria maculans*. *Fungal Genet. Biol.* **53**, 50–58.

Elliotte, C.E., Gardnier, D.M., Thomas, G., Cozijnsen, A., Van de Wouw, A. and Howlett, B.J. (2007) Production of the toxin sirodesmin PL by *Leptosphaeria maculans* during infection of *Brassica napus*. *Mol. Plant Pathol.* **8**, 791–802.

Emanuelsson, O., Nielsen, H., Brunak, S. and Heijne, G.V. (2000) Predicting subcellular localization of proteins based on their N-terminal amino acid sequence. *J. Mol. Biol.* **300**, 1005–1016.

Finn, R.D., Bateman, A., Clements, J., Coggill, P., Eberhardt, R.Y., Eddy, S.R., Heger, A., Hetherington, K., Holm, L., Mistry, J., Sonnhammer, E.L.L., Tate, J. and Punta, M. (2014) The Pfam protein families database. *Nucleic Acids Res.* **42**, D222–D230.

Fischer, S., Brunk, B.P., Chen, F., Gao, X., Harb, O.S., Iodice, J.B., Shanmugam, D., Roos, D.S. and Stoeckert, C.J., Jr. (2011) Using OrthoMCL to assign proteins to OrthoMCL-DB groups or to cluster proteomes into new ortholog groups. *Curr. Protoc. Bioinformatics, Andreas D. Baxevanis [et al.]*, Chapter 6, Unit 6 12 11–19.

Fitt, B.D.L., Brun, H., Barbetti, M.J. and Rimmer, S.R. (2006) World-wide importance of phoma stem canker (*Leptosphaeria maculans* and *L. biglobosa*) on oilseed rape (*Brassica napus*). *Eur. J. Plant Pathol.* **114**, 3–15.

Fudal, I., Ross, S., Gout, L., Blaise, F., Kuhn, M.L., Eckert, M.R., Cattolico, L., Bernard-Samain, S., Balesdent, M.H. and Rouxel, T. (2007) Heterochromatin-like regions as ecological niches for avirulence genes in the *Leptosphaeria maculans* genome: map-based cloning of AvrLm6. *Mol. Plant–Microbe Interact.* **20**: 459–470.

Ghanbarnia, K., Fudal, I., Larkan, N.J., Links, M.G., Balesdent, M.H., Profotova, B., Fernando, W.G., Rouxel, T. and Borhan, M.H. (2015) Rapid identification of the *Leptosphaeria maculans* avirulence gene AvrLm2 using an intraspecific comparative genomics approach. *Mol. Plant Pathol.* **16**, 699–709.

Gijzen, M. and Nurnberger, T. (2006) Nep1-like proteins from plant pathogens: recruitment and diversification of the NPP1 domain across taxa. *Phytochemistry*, **67**, 1800–1807.

Glazebrook, J. (2005) Contrasting mechanisms of defense against biotrophic and necrotrophic pathogens. *Annu. Rev. Phytopathol.* **43**, 205–227.

Gout, L., Fudal, I., Kuhn, M.L., Blaise, F., Eckert, M., Cattolico, L., Balesdent, M.H. and Rouxel, T. (2006) Lost in the middle of nowhere: the AvrLm1 avirulence gene of the Dothideomycete *Leptosphaeria maculans*. *Mol. Microbiol.* **60**, 67–80.

Guyon, K., Balague, C., Roby, D. and Raffaele, S. (2014) Secretome analysis reveals effector candidates associated with broad host range necrotrophy in the fungal plant pathogen *Sclerotinia sclerotiorum*. *BMC Genomics*, **15**, 336.

Jacobson, E.S. (2000) Pathogenic roles for fungal melanins. *Clin. Microbiol. Rev.* **13**, 708–717.

Kanehisa, M. and Goto, S. (2000) KEGG: Kyoto encyclopedia of genes and genomes. *Nucleic Acids Res.* **28**, 27–30.

Kanehisa, M., Goto, S., Sato, Y., Kawashima, M., Furumichi, M. and Tanabe, M. (2014) Data, information, knowledge and principle: back to metabolism in KEGG. *Nucleic Acids Res.* **42**, D199–D205.

Katagiri, F. and Tsuda, K. (2010) Understanding the plant immune system. *Mol. Plant–Microbe Interact.* **23**, 1531–1536.

Khaldi, N., Seifuddin, F.T., Turner, G., Haft, D., Nierman, W.C., Wolfe, K.H. and Fedorova, N.D. (2010) SMURF: genomic mapping of fungal secondary metabolite clusters. *Fungal Genet. Biol.* **47**, 736–741.

Kim, S.T., Kim, S.G., Hwang, D.H., Kang, S.Y., Kim, H.J., Lee, B.H. and Kang, K.Y. (2004) Proteomic analysis of pathogen-responsive proteins from rice leaves induced by rice blast fungus, *Magnaporthe grisea*. *Proteomics*, **4**, 3569–3578.

Krogh, A., Larsson, B., von Heijne, G. and Sonnhammer, E.L. (2001) Predicting transmembrane protein topology with a hidden Markov model: application to complete genomes. *J. Mol. Biol.* **305**, 567–580.

Laluk, K. and Mengiste, T. (2010) Necrotroph attacks on plants: wanton destruction or covert extortion? *The Arabidopsis Book*, **8**, e0136. doi:10.1199/tab.0136.

Larkan, N.J., Lydiate, D.J., Parkin, I.A.P., Nelson, M.N., Epp, D.J., Cowling, W.A., Rimmer, S.R. and Borhan, M.H. (2013) The *Brassica napus* blackleg resistance gene LepR3 encodes a receptor-like protein triggered by the *Leptosphaeria maculans* effector AVRLM1. *New Phyto.* **197**, 595–605.

Larkan, N.J., Lydiate, D.J., Yu, F., Rimmer, S.R. and Borhan, M.H. (2013) Co-localisation of the blackleg resistance genes Rlm2 and LepR3 on *Brassica napus* chromosome A10. *BMC Plant Biol.* **14**, 387.

Larkan, N.J., Ma, L. and Borhan, M.H. (2015) The *Brassica napus* receptor-like protein RLM2 is encoded by a second allele of the LepR3/Rlm2 blackleg resistance locus. *Plant Biotechnol. J.* **13**, 983–992.

Levasseur, A., Drula, E., Lombard, V., Coutinho, P.M. and Henrissat, B. (2013) Expansion of the enzymatic repertoire of the CAZy database to integrate auxiliary redox enzymes. *Biotechnol. Biofuels*, **6**, 41.

Liebrand, T.W., van den Burg, H.A. and Joosten, M.H. (2014) Two for all: receptor-associated kinases SOBIR1 and BAK1. *Trends Plant Sci.* **19**, 123–132.

Love, M.L., Huber, W. and Anders, S.(2014) Moderated estimation of fold change and dispersion for RNA-seq data with DESeq2. *Genome Biol.* **15**, 550.

Lowe, R.G., Cassin, A., Grandaubert, J., Clark, B.L., Van de Wouw, A.P., Rouxel, T. and Howlett, B.J. (2014) Genomes and transcriptomes of partners in plant–fungal interactions between canola (*Brassica napus*) and two *Leptosphaeria* species. *PLoS One*, **9**, e103098.

Ma, L. and Borhan, M.H. (2015) The receptor-like kinase SOBIR1 interacts with *Brassica napus* LepR3 and is required for *Leptosphaeria maculans* AvrLm1-triggered immunity. *Front Plant Sci.* **6**, 933. DOI=10.3389/fpls.2015.00933.

Ma, L., Houterman, P.M., Gawehns, F., Cao, L., Sillo, F., Richter, H., Clavijo-Ortiz, M.J., Schmidt, S.M., Boeren, S., Vervoort, J., Cornelissen, B.J., Rep, M. and Takken, F.L. (2015) The AVR2-SIX5 gene pair is required to activate I-2-mediated immunity in tomato. *New Phytol.* **208**, 507–518.

Ma, L., Lukasik, E., Gawehns, F. and Takken, F.L. (2012) The use of agroinfiltration for transient expression of plant resistance and fungal effector proteins in *Nicotiana benthamiana* leaves. *Methods Mol. Biol.* **835**, 61–74.

Malinovsky, F.G., Fangel, J.U. and Willats, W.G.T. (2014) The role of the cell wall in plant immunity. *Frontiers in Plant Science*, doi:10.3389/fpls.2014.00178.

Masuda, D., Ishida, M., Yamaguchi, K., Yamaguchi, I., Kimura, M. and Nishiuchi, T. (2007) Phytotoxic effects of trichothecenes on the growth and morphology of *Arabidopsis thaliana*. *J. Exp. Bot.* **58**, 1617–1626.

Metzker, M.L. (2010) Sequencing technologies – the next generation. *Nat. Rev. Genet.* **11**, 31–46.

Mikkelsen, M.D., Naur, P. and Halkier, B.A. (2004) Arabidopsis mutants in the C-S lyase of glucosinolate biosynthesis establish a critical role for indole-3-acetaldoxime in auxin homeostasis. *Plant J.* **37**, 770–777.

Mumm, R., Burow, M., Bukovinszkine'kiss, G., Kazantzidou, E., Wittstock, U., Dicke, M. and Gershenzon, J. (2008) Formation of simple nitriles upon glucosinolate hydrolysis affects direct and indirect defense against the specialist herbivore, *Pieris rapae. J. Chem. Ecol.* **34**, 1311–1321.

Nakagawa, T., Suzuki, T., Murata, S., Nakamura, S., Hino, T., Maeo, K., Tabata, R., Kawai, T., Tanaka, K., Niwa, Y., Watanabe, Y., Nakamura, K., Kimura, T. and Ishiguro, S. (2007) Improved Gateway binary vectors: high-performance vectors for creation of fusion constructs in transgenic analysis of plants. *Biosci. Biotechnol. Biochem.* **71**, 2095–2100.

Parlange, F., Daverdin, G., Fudal, I., Kuhn, M.L., Balesdent, M.H., Blaise, F., Grezes-Besset, B. and Rouxel, T. (2009) *Leptosphaeria maculans* avirulence gene AvrLm4-7 confers a dual recognition specificity by the Rlm4 and Rlm7 resistance genes of oilseed rape, and circumvents Rlm4-mediated recognition through a single amino acid change. *Mol. Microbiol.* **71**, 851–863.

Pedersen, C., Themmat, E.V.L., McGuffin, L., Abbott, J.C., Burgis, T.A., Barton, G., Bindschedler, L.V., Lu, X., Maekawa, T., Wessling, R., Cramer, R., Thordal-Christensen, H., Panstruga, R. and Spanu, P.D. (2012) Structure and evolution of barley powdery mildew effector candidates. *BMC Genomics*, **13**, 694.

Peng, Y., Bartley, L.E., Chen, X., Dardick, C., Chern, M., Ruan, R., Canlas, P.E. and Ronald, P.C. (2008) OsWRKY62 is a negative regulator of basal and Xa21-mediated defense against *Xanthomonas oryzae* pv. oryzae in rice. *Mol. Plant*, **1**, 446–458.

Petersen, T.N., Brunak, S., Heijne, G.V. and Nielsen, H. (2011) SignalP 4.0: discriminating signal peptides from transmembrane regions. *Nat. Methods*, **8**, 785–786.

Pierleoni, A., Martelli, P.L. and Casadio, R. (2008) PredGPI: a GPI anchor predictor. *BMC Bioinformatics*, **9**, 392.

Pieterse, C.M., Van der Does, D., Zamioudis, C., Leon-Reyes, A. and Van Wees, S.C. (2012) Hormonal modulation of plant immunity. *Annu. Rev. Cell Dev. Biol.* **28**, 489–521.

Postma, J., Liebrand, T.W.H., Bi, G., Evrard, A., Bye, R.R., Mbengue, M., Joosten, M.H.A.J. and Robatzek, S. (2015) The Cf-4 receptor-like protein associates with the BAK1 receptor-like kinase to initiate receptor endocytosis and plant immunity. *bioRxiv* doi: http://dx.doi.org/10.1101/019471.

Qiu, D., Xiao, J., Xie, W., Liu, H., Li, X., Xiong, L. and Wang, S. (2008) Rice gene network inferred from expression profiling of plants overexpressing OsWRKY13, a positive regulator of disease resistance. *Mol. Plant*, **1**, 538–551.

Qutob, D., Kamoun, S. and Gijzen, M. (2002) Expression of a *Phytophthora sojae* necrosis-inducing protein occurs during transition from biotrophy to necrotrophy. *Plant J.* **32**, 361–373.

Raman, H., Raman, R. and Larkan, N. (2013) Genetic dissection of Blackleg Resistance Loci in rapeseed (*Brassica napus* L.) In: *Plant Breeding from Laboratories to Fields.* (Andersen, S. B., ed.). Rijeka, Croatia: InTech, pp. 85–120.

Robert-Seilaniantz, A., Grant, M. and Jones, J.D. (2011) Hormone crosstalk in plant disease and defense: more than just jasmonate–salicylate antagonism. *Annu. Rev. Phytopathol.* **49**, 317–343.

Rouxel, T. and Balesdent, M.H. (2005) The stem canker (blackleg) fungus, *Leptosphaeria maculans*, enters the genomic era. *Mol. Plant Pathol.* **6**, 225–241.

Rouxel, T., Grandaubert, J., Hane, J.K., Hoede, C., van de Wouw, A.P., Couloux, A., Dominguez, V., Anthouard, V., Bally, P., Bourras, S., Cozijnsen, A.J., Ciuffetti, L.M., Degrave, A., Dilmaghani, A., Duret, L., Fudal, I., Goodwin, S.B., Gout, L., Glaser, N., Linglin, J., Kema, G.H., Lapalu, N., Lawrence, C.B., May, K., Meyer, M., Ollivier, B., Poulain, J., Schoch, C.L., Simon, A., Spatafora, J.W., Stachowiak, A., Turgeon, B.G., Tyler, B.M., Vincent, D., Weissenbach, J., Amselem, J., Quesneville, H., Oliver, R.P., Wincker, P., Balesdent, M.H. and Howlett, B.J. (2011) Effector diversification within compartments of the *Leptosphaeria maculans* genome affected by repeat-induced point mutations. *Nat. Commun.* **2**, 202.

Šašek, V., Novakova, M., Jindrichova, B., Boka, K., Valentova, O. and Burketova, L. (2012) Recognition of avirulence gene AvrLm1 from hemibiotrophic ascomycete *Leptosphaeria maculans* triggers salicylic acid and ethylene signaling in *Brassica napus. Mol. Plant–Microbe Interact.* **25**, 1238–1250.

Scharf, D.H., Heinekamp, T. and Brakhage, A. (2014) Human and plant fungal pathogens: the role of secondary metabolites. *PLoS Pathog.* **10**, e1003859.

Shimono, M., Sugano, S., Nakayama, A., Jiang, C.J., Ono, K., Toki, S. and Takatsuji, H. (2007) Rice WRKY45 plays a crucial role in benzothiadiazole-inducible blast resistance. *Plant Cell*, **19**, 2064–2076.

Sperschneider, J., Dodds, P.N., Gardiner, D.M., Manners, J.M., Singh, K.B. and Taylor, J.M. (2015) Advances and challenges in computational prediction of effectors from plant pathogenic fungi. *PLoS Pathog.* **11**, e1004806.

Stotz, U.H., Sawada, Y., Shimada, Y., Hirai, M.Y., Sasaki, E., Krischke, M., Brown, P.D., Saito, K. and Kamiya, Y. (2011) Role of camalexin, indole glucosinolates, and side chain modification of glucosinolate-derived isothiocyanates in defense of Arabidopsis against *Sclerotinia sclerotiorum. Plant J.* **67**, 81–93.

Stotz, H.U., Mitrousia, G.K., de Wit, P.J.G.M. and Fitt, B.D.L. (2014) Effector-triggered defence against apoplastic fungal pathogens. *Trends in Plant Science*, **19**, 491–500.

Thimm, O., Bläsing, O., Gibon, Y., Nagel, A., Meyer, S., Krüger, P., Selbig, J., Müller, L.A., Rhee, S.Y. and Stitt, M. (2004) MAPMAN: a user-driven tool to display genomics data sets onto diagrams of metabolic pathways and other biological processes. *Plant J.* **37**, 914–939.

Utermark, J. and Karlovsky, P. (2008) Genetic transformation of filamentous fungi by *Agrobacterium tumefaciens*. In: *Nature Protocol Exchange*. Nature Publishing Group. URL: http://www.nature.com/protocolexchange/protocols/427.

Van de Wouw, A.P., Lowe, R.G., Elliott, C.E., Dubois, D.J. and Howlett, B.J. (2014) An avirulence gene, AvrLmJ1, from the blackleg fungus, *Leptosphaeria maculans*, confers avirulence to *Brassica juncea* cultivars. *Mol. Plant Pathol.* **15**, 523–530.

Volodarsky, D., Leviatan, N., Otcheretianski, A. and Fluhr, R. (2009) HORMONOMETER: a tool for discerning transcript signatures of hormone action in the Arabidopsis transcriptome. *Plant Physiol.* **150**, 1796–1805.

Wang, H., Hao, J., Chen, X., Hao, Z., Wang, X., Lou, Y., Peng, Y. and Guo, Z. (2007) Overexpression of rice WRKY89 enhances ultraviolet B tolerance and disease resistance in rice plants. *Plant Mol. Biol.* **65**, 799–815.

Wang, Y., Kim, S.G., Wu, J., Huh, H.H., Lee, S.J., Rakwal, R., Agrawal, G.K., Park, Z.Y., Young Kang, K. and Kim, S.T. (2013) Secretome analysis of the rice bacterium *Xanthomonas oryzae* (Xoo) using in vitro and in planta systems. *Proteomics*, **13**, 1901–1912.

Wang, Y., Kwon, S.J., Wu, J., Choi, J., Lee, Y.H., Agrawal, G.K., Tamogami, S., Rakwal, R., Park, S.R., Kim, B.G., Jung, K.H., Kang, K.Y., Kim, S.G. and Kim, S.T. (2014) Transcriptome analysis of early responsive genes in rice during *Magnaporthe oryzae* infection. *Plant Pathol. J.* **30**, 343–354.

Wang, Z.Y. (2012) Brassinosteroids modulate plant immunity at multiple levels. *Proc. Natl. Acad. Sci. USA*, **109**, 7–8.

West, J.S., Kharbanda, P.D., Barbetti, M.J. and Fitt, B.D.L. (2001) Epidemiology and management of *Leptosphaeria maculans* (phoma stem canker) on oilseed rape in Australia, Canada and Europe. *Plant Pathol.* **50**, 10–27.

Westermann, A.J., Gorski, S.A. and Vogel, J. (2012) Dual RNA-seq of pathogen and host. *Nat. Rev. Microbiol.* **10**, 618–630.

Wrzaczek, M., Brosche, M., Salojarvi, J., Kangasjarvi, S., Idanheimo, N., Mersmann, S., Robatzek, S., Karpiński, S., Karpińska, B. and Kangasjärvi, J. (2010) Transcriptional regulation of the CRK/DUF26 group of receptor-like protein kinases by ozone and plant hormones in Arabidopsis. *BMC Plant Biol.* **10**, 95.

Yin, Y., Mao, X., Yang, J., Chen, X., Mao, F. and Xu, Y. (2012) dbCAN: a web resource for automated carbohydrate-active enzyme annotation. *Nucleic Acids Res.* **40**, W445–W451.

Zaparoli, G., Barsottini, M.R., de Oliveira, J.F., Dyszy, F., Teixeira, P.J., Barau, J.G., Garcia, O., Costa-Filho, A.J., Ambrosio, A.L., Pereira, G.A. and Dias, S.M. (2011) The crystal structure of necrosis- and ethylene-inducing protein 2 from the causal agent of cacao's Witches' Broom disease reveals key elements for its activity. *Biochemistry*, **50**, 9901–9910.

Zhang, J., Peng, Y. and Guo, Z. (2008) Constitutive expression of pathogen-inducible OsWRKY31 enhances disease resistance and affects root growth and auxin response in transgenic rice plants. *Cell Res.* **18**, 508–521.

SUPPORTING INFORMATION

Additional Supporting Information may be found in the online version of this article at the publisher's website:

Fig. S1 RNA-sequencing quality assessment. Variation within the four replicates was determined from the following: (A) density plots; red arrows indicate that the density of the counts in the third replicate for the time points 4, 6 and 8 days after inoculation (dai) was distinctly different from that for the same time points in other replicates; (B) clustering of the sample-to-

sample distances; closely grouped replicates within the clusters are indicated by red circles; (C) the MA plot between two biological replicates per time point; M values (the log fold change), the log of the ratio of level counts for each gene between two biological replicates per time point; A values (the log-average), the average level counts for each gene across two biological replicates per time point. Genes with similar expression levels in two biological replicates per time point will appear around the horizontal line ($y = 0$). The third replicates of each time point that were distinctly different from the corresponding points in other replicates are marked by red boxes.

Fig. S2 Expression profiles of *Leptosphaeria maculans* (*Lm*) secondary metabolite-related genes are presented as green (low) or red (high). NS, non-significant.

Fig. S3 Lema_T086540.1 with homology to the *Fusarium* effector Six5. (A) Location of the gene in the AT-rich region of the *Leptosphaeria maculans* genome. (B) Expression profile of T086540.1 grown *in vitro* and during *Brassica napus* infection. (C) Conserved cysteine residues between *Six5* and Lema_T086540.1 are marked by red arrows. *Significant at 0.05 probability level. ***Significant at 0.001 probability level.

Fig. S4 (A) Quantitative reverse transcription-polymerase chain reaction (RT-PCR) analysis of the *NLP* gene in the wild-type and *NLP* silencing line NLP-SL1. RT-PCR products obtained from RNA isolated from *Brassica napus* cv. Topas at 6 days after inoculation with the wild-type isolate 00-100 and *NLP* silencing line NLP-SL1. *NLP* gene expression levels are normalized to that of actin. Values are means ± standard error (SE) of triplicate reactions of three independent biological samples. Significant differences are represented by three asterisks ($P < 0.001$). (B) The *NLP-SL1* silencing line showed a slightly reduced growth rate on V8 medium. Wild-type *L. maculans* 00-100 and one of the *NLP* silencing lines *NLP-SL1* were grown on a V8 medium plate and photographs were taken at 7 days after inoculation.

Fig. S5 Expression profile of AtSOBIR1 orthologues in *Brassica napus*.

Fig. S6 Expression profile of *Leptosphaeria maculans* nitrile-specifier protein 5 (NSP5), CYP79B2 and SUPERROOT1 (SUR1) at different time points.

Table S1 Summary of RNA-sequencing (RNA-seq) reads mapped to the *Brassica napus* (A) and *Leptosphaeria maculans* (B) reference genomes.

Table S2 List of small secreted protein (SSP)-encoding genes as the most likely set of *Leptosphaeria maculans* predicted effectors that were found to be differentially expressed [false discovery rate-Benjamini–Hochberg (FDR-BH) of less than 0.05] based on DESeq2 software.

Table S3 Primer combinations for the amplification of effector candidate-related genes.